Dendrimer-Modified Magnetic Nanoparticles Enhance Efficiency of Gene Delivery System

Bifeng Pan,[1] Daxiang Cui,[1] Yuan Sheng,[2] Cengiz Ozkan,[3] Feng Gao,[1] Rong He,[1] Qing Li,[1] Ping Xu,[1] and Tuo Huang[1]

[1]Department of Bio-Nano-Science and Engineering, National Key Laboratory of Nano/Micro Fabrication Technology, Key Laboratory for Thin Film and Microfabrication of Ministry of Education, Institute of Micro-Nano Science and Technology, Shanghai Jiao Tong University; [2]Breast Cancer Therapy Center of Changhai Hospital, Second Military Medical University, Shanghai, People's Republic of China; and [3]Department of Mechanical Engineering, University of California at Riverside, Riverside, California

Abstract

Magnetic nanoparticles (MNP) with a diameter of 8 nm were modified with different generations of polyamidoamine (PAMAM) dendrimers and mixed with antisense *survivin* oligodeoxynucleotide (asODN). The MNP then formed asODN-dendrimer-MNP composites, which we incubated with human tumor cell lines such as human breast cancer MCF-7, MDA-MB-435, and liver cancer HepG2 and then analyzed by 3-(4,5-dimethylthiazol-2-yl)-2,5-diphenyltetrazolium bromide, quantitative reverse transcription-PCR, Western blotting, laser confocal microscopy, and high-resolution transmission electron microscopy. Results showed that the asODN-dendrimer-MNP composites were successfully synthesized, can enter into tumor cells within 15 min, caused marked down-regulation of the *survivin* gene and protein, and inhibited cell growth in dose- and time-dependent means. No.5 generation of asODN-dendrimer-MNP composites exhibits the highest efficiency for cellular transfection and inhibition. These results show that PAMAM dendrimer-modified MNPs may be a good gene delivery system and have potential applications in cancer therapy and molecular imaging diagnosis. [Cancer Res 2007;67(17):8156–63]

Introduction

Several promising nanoparticle delivery systems have been proposed for gene therapy (1–4). For example, superparamagnetic iron oxide nanoparticles have been recognized as a promising tool for the site-specific delivery of drugs and diagnostics agents (5–7). Magnetic nanoparticles (MNP) have been widely explored to have potentials in applications, such as hyperthermia (8), magnetic resonance imaging contrast agent (9), tissue repair (10), immunoassay (11), drug/gene delivery (12), and cell separation (13). However, few reports are closely associated with use of MNPs as gene transfection vector for cancer therapy.

As you know, antisense strategy is an effective gene therapy for cancer. A lot of reports have confirmed that antisense oligonucleotides can bind start location of mRNA translation inside cells, block translation of target RNA into target protein, and finally suppress cellular proliferation (14–16). However, antisense therapy is still restricted in application of clinical therapy because of two existing problems, such as rapid degradation by exonuclease or endonuclease and poor diffusion across the cell membrane (17–19). Although some methods, such as chemically modified oligonucleotides, oligonucleotides bound to virus and synthetic carriers, and small interfering RNA, have been explored to solve these problems (20, 21), so far no optimal solution is established. Therefore, looking for more effective alternative delivery system for antisense nucleotides is the key to solve the present problems. As the advance of nanotechnology, new nanomaterials are being continuously fabricated, which makes it possible that one kind of novel nanomaterials acts as the delivery system for antisense therapy.

Dendrimers are a relatively novel class of polymers with highly ordered structure (22, 23). The accretion of functional groups, symmetry perfection, nanosize, and internal cavities provides these novel dendritic nanocomposites many potential applications in biochemistry (24), gene therapy (25), and nanomedicine (26). Dendrimer should become one kind of good nonviral synthetic vectors because of the advantages of safety, simplicity of use, and ease of mass production compared with viral vectors with an inherent risk for clinical use (24, 25). Nanoparticles coated with dendrimer can alter the charge, functionality, and reactivity and enhance the stability and dispersibility of the nanoparticles (27–29).

In this study, we fully used the advantages of MNPs and polyamidoamine (PAMAM) dendrimers and explored to solve two problems associated with gene therapy of antisense oligonucleotides, such as poor diffusion across cell membrane and rapid degradation by exonuclease or endonuclease, by fabricating nanoscale delivery system composed of MNPs covered with different generation of PAMAM dendrimers [dendrimer-modified MNPs (dMNP)]. To confirm the feasibility of synthesized nanoscale delivery system, we selected *survivin* gene as research target (30–32). The synthesized dMNP composites were used to complex with antisense *survivin* oligodeoxynucleotides (asODN). Then, we investigated gene transfection efficacy, uptake mechanism, and biological effects of the dMNPs with breast cancer cells, such as MCF-7 and MDA-MB-435 cell lines, and liver cancer HepG2 cell line. Our results showed that the surface dendritic structure of the MNPs allows gene to attach to the surface of dMNPs and markedly enhanced the gene delivery efficiency. The system renders the possibility to serve as a universal transmembrane carrier for intracellular gene and drug delivery and imaging applications.

Materials and Methods

Cell lines and reagents. Human breast cancer cell lines (MCF-7 and MDA-MB-435), liver cancer HepG2 cell line, human prostate cancer LNCaP cell line, and HL-60 cell line were obtained from the American Type Culture

Requests for reprints: Daxiang Cui, Department of Bio-Nano-Science and Engineering, National Key Laboratory of Nano/Micro Fabrication Technology, Key Laboratory for Thin Film and Microfabrication of Ministry of Education, Institute of Micro-Nano Science and Technology, Shanghai Jiao Tong University, 1954 Huashan Road, Shanghai 200030, People's Republic of China. Phone: 86-21-62933291; Fax: 86-21-62933291; E-mail: dxcui@sjtu.edu.cn.

doi:10.1158/0008-5472.CAN-06-4762

Collection. Methacrylate, ethylenediamine, ferrous chloride, 3-aminopropyltrimethoxysilane (APTS), FITC dye, and ferric chloride were purchased from Sigma Chemical Co. 3-(4,5-Dimethylthiazol-2-yl)-2,5-diphenyltetrazolium bromide (MTT), FCS, RPMI 1640, DMSO, and all reagents for electrophoresis were obtained from Life Technologies. Rabbit anti-human polyclonal antibody against *survivin*, β-actin antibody, and horseradish peroxidase (HRP)-conjugated goat anti-rabbit secondary antibody were from Invitrogen Co.

PCR primers and antisense ODNs. PCR primers were as follows: *survivin* gene, 5′-GTGAATTTTTGAAACTGGACAG-3′ (forward) and 5′-CCTTTCCTAAGACATTGCTAAG-3′ (reverse; amplification fragment is 240 bp); glyceraldehyde-3-phosphate dehydrogenase (GAPDH; internal control), 5′-CCACCCATGGCAAATTCCATGGCA-3′ (forward) and 5′-TCTAGACGGCAGGTCAGGTCCACC-3′ (reverse; product length is 180 bp). asODN sequence was complementary to the first five codons of human *survivin* mRNA (5′-CCCAGCCTTCCAGCTCCTTG-3′), and a negative control ODN [nonsense ODN (nsODN)] sequence was not complementary to the *survivin* mRNA (5′-CTGGCCGCTGGATTCCTGCT-3′). PCR primers, oligonucleotides, and FITC-labeling oligonucleotides were designed and synthesized by Shanghai Sangon Biotech.

Preparation of MNPs. MNPs were prepared under various reaction conditions by coprecipitation of Fe^{2+} and Fe^{3+} in the presence of NaOH (27, 28). Finally, MNPs were dispersed in PBS (pH 7.4).

Growth of PAMAM dendrimer on magnetic surface. dMNPs were prepared according to our previous works as shown in Fig. 1 (28, 29). Briefly, magnetic methanol solution was treated by ultrasonic waves for 30 min. Excessive APTS $[NH_2(CH_2)_3\text{-Si-}(OCH_3)_3]$ was added with rapid stirring for 7 h. The resulting solution was washed with methanol five times by magnetic separation. APTS-coated MNPs were terminated with amine groups and dispersed in methanol. G_0 dMNP represents the MNPs modified with only APTS. Dendrimer generation was initiated with G_0 methanol solution. Excessive methacrylate was added and the suspension was immersed in an ultrasonicating water bath at room temperature for 7 h. The particles were then collected magnetically and rinsed with methanol five times by magnetic separation. After rinsing, excessive ethylenediamine was then added and the suspension was immersed in an ultrasonicating water bath at room temperature for 3 h. The particles were rinsed with methanol five times by magnetic separation. Stepwise growth using methacrylate and ethylenediamine was repeated until the desired number of generations from 1.0 to 5.0 ($G_{1.0}$-$G_{5.0}$) was achieved.

Characterization of dMNPs. To characterize the samples, portions of the dMNP suspensions were dried at 80°C under vacuum. The average size was estimated using a high-resolution transmission electron microscope (HR-TEM; JEM 4010, JEOL). Fourier transformation-IR (FT-IR) spectra of suspensions were obtained using a FT-IR spectrophotometer (Avatar 360, Nicolet). Thermogravity analysis (TGA) measurement was done by TGA

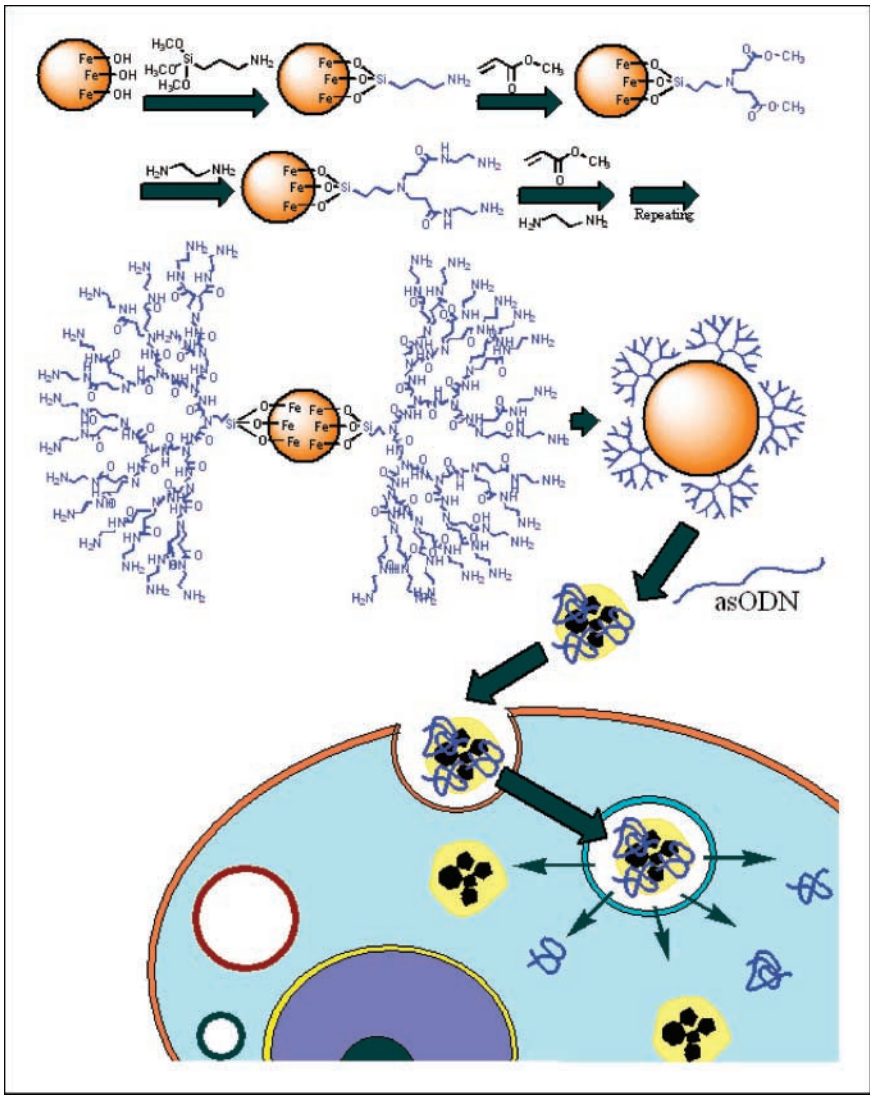

Figure 1. Growth of PAMAM dendrimer on the surface of MNPs for nonviral gene transfection based on complexation with an asODN. Nine steps are shown in the process: APTS was added to form amine-terminated MNPs (G_0 dMNP), excessive methacrylate was added to get a ester-terminated MNPs, ethylenediamine was added to form amine-terminated $G_{1.0}$ dMNP, methacrylate and ethylenediamine were added alternately to get dMNP with generation from 1.0 to 5.0, complexation between dMNP and asODN, adsorption of dMNP-asODN complexes onto cancer cells surface, dMNP-asODN complexes were endocytosed by cancer cells, endosome-containing dMNP-asODN complexes were located around the nucleus, and dMNP and asODN escaped from the endosome into cytoplasm.

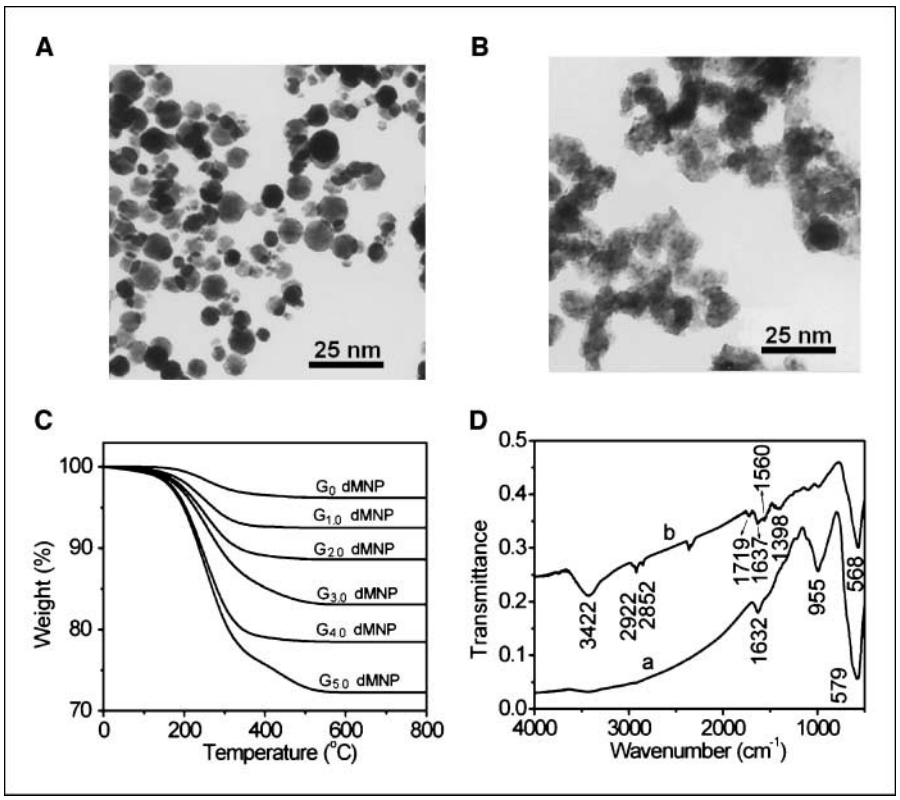

Figure 2. *A* and *B,* HR-TEM images of MNPs before and after dendrimer modification (MNPs and $G_{5.0}$ dMNPs, respectively). *C,* TGA curves of dMNPs. *D,* FT-IR spectra of MNPs and $G_{5.0}$ dMNPs.

2850 thermogravimetric analyzer (TA Instruments) under N_2 in the temperature range 30°C to 700°C with an increasing rate of 5°C/min.

Preparation of dMNP-asODN composites. *Survivin* asODN was mixed with dMNP in RPMI 1640 without FCS under the condition of the charge ratio of 10:1 (dMNP/asODN) and incubated for 30 min at room temperature. For confocal microscopy observation, FITC-labeled asODN was used to form dMNP-FITC-asODN complex. Control experiments were carried out by mixing dMNP and nsODN (dMNP-nsODN).

Electrophoretic shift assay and ζ potential analysis. dMNPs (0.2 μg) at different generation were mixed with 5.0 nmol asODN or nsODN, and 5.0 nmol of free asODN and nsODN were used as control and added to a 1% agarose gel in Tris-acetic acid-EDTA buffer containing ethidium bromide. The gel was run for 1 h at 90 V and then photographed under UV light using a UVP gel documentation system. Each sample was run in duplicate. ζ Potential was measured with Zetasizer 2000 instruments (Malvern Co.).

Cell culture and microscopy observation. Human breast cancer MCF-7 and MDA-MB-435 cell lines, liver cancer HepG2 cell line, human prostate cancer LNCaP cell line, and HL-60 cells were cultured for 24 h in RPMI 1640 containing 1×10^5 milliunits/mL penicillin and 0.1 mg/mL streptomycin supplemented with 10% (v/v) FCS at 37°C in a humidified 5% CO_2 incubator. FITC-labeled asODN-dMNPs were mixed fully with 0.1% bovine serum albumin (BSA) and then added into the cultured cells. These cells were collected and observed with laser confocal microscopy. Partial collected cells were embedded and made into TEM specimens and then observed via HR-TEM.

For quantitative intercellular assay, fluorescence of cell growth medium supernatant was detected after the incubation of cancer cells with dMNP-FITC-asODN. The uptake rate (%) was measured by the following equation:

$$\text{Uptake rate } (\%) = [1 - (I_{\text{test}}/I_{\text{control}})] \times 100 \qquad \text{(A)}$$

Here, I_{control} is the fluorescence intensity of the same cell culture medium containing dMNP-FITC-asODN and I_{test} is the fluorescence of supernatant after incubation of cell with dMNP-FITC-asODN.

Cell viability and proliferation assays. Cell viability and proliferation were measured by MTT assays. Every well in the 96-well plate was added into 180 μL RPMI 1640 and 5,000 cells and incubated in a humidified 5% CO_2 balanced air incubator at 37°C for 24 h. Except from control wells, the remaining well was added into 20 μL dMNP-asODN composites and continued to culture for 72 h and then each well was added into 0.05 mL MTT solution and continued to culture for 2 h. Then, each well was added into 0.05 mL DMSO to dissolve the formed crystals. The 96-well microplate was read at 570 nm on an ELISA plate reader and the percentage of viability was calculated (33). The inhibition of cell proliferation can be calculated by the following equation:

$$\text{Inhibition of cell proliferation } (\%) = \left(1 - \frac{A_{570(\text{test})}}{A_{570(\text{control})}}\right) \times 100 \qquad \text{(B)}$$

where $A_{570(\text{test})}$ is absorbance intensity at 570 nm in the presence of dMNP-asODN complex and $A_{570(\text{control})}$ is absorbance intensity at 570 nm in the absence of dMNP-asODN complex.

Semiquantitative reverse transcription-PCR analysis. Cellular total RNAs were extracted out by using Total RNA Extraction kit according to the manufacturer's instructions. Single-stranded cDNA was synthesized with oligo(dT) primer in a 20 μL reaction from 5 μg of total RNA using SuperScript Preamplification System for First-Strand cDNA Synthesis System (Promega Co.) and diluted up to 80 μL. PCR was then done with 1 μL cDNA for 1 cycle of 94°C for 2 min followed by 30 cycles of 94°C for 30 s, 60°C for 30 s, and 72°C for 3 min using gene-specific primers and Taq polymerase. PCR products were analyzed on 1% agarose gel electrophoresis with ethidium bromide, and GAPDH was used as internal control to confirm equal amount of the templates.

Western blot analysis. Cells were lysed in protein lysis buffer [50 mmol/L Tris (pH 7.4), 150 mmol/L NaCl, 1 mmol/L EDTA, 1 mmol/L EGTA, 5% 2-mercaptoethanol, 1% NP40, 0.25% sodium deoxycholate, 5 μg/mL leupeptin, 5 μg/mL aprotinin, 10 μg/mL soybean trypsin inhibitor, 0.2 mmol/L phenylmethylsulfonyl fluoride]. Protein concentrations were determined using the Bradford method. Equal amounts of sample lysate

were separated by SDS-PAGE and electrophoretically transferred onto polyvinylidene difluoride membranes (Millipore). The membrane was blocked with 0.1% BSA in TBST buffer [20 mmol/L Tris (pH 7.4), 150 mmol/L NaCl, 0.1% Tween 20] and incubated overnight at 4°C with rabbit anti-human polyclonal antibody against *survivin*. Subsequently, the membrane was washed with TBST buffer and incubated with HRP-conjugated secondary antibody. Enhanced chemiluminescence kits were used (Amersham). β-Actin was used as a negative control (34).

Data analysis. All data are presented in this article as mean result ± SD. Statistical differences were evaluated using the *t* test and considered significant at $P < 0.05$ level. All figures shown in this article were obtained from three independent experiments with similar results.

Results

Characterization of dMNPs. Figure 2 shows the results of different generation of dMNPs characterized by HR-TEM, TGA, and FT-IR. As shown in Fig. 2*A*, the synthesized MNPs were quasi-spherical with an average diameter of 8.0 nm and were dispersed very evenly in liquid. As shown in Fig. 2*B*, dMNPs were dispersed very well with average diameter of 20 to 40 nm, which also implies that the strong repulsion force existed among these dMNPs. The dendrimer coating layer on the surface of MNPs can be clearly observed by HR-TEM and also can be further confirmed by TGA analysis as shown in Fig. 2*C* and FT-IR spectra analysis as shown in Fig. 2*D*. The grafted dendrimer content of the dMNP can be calculated from TGA from the weight loss between 20°C and 800°C (Fig. 2*C*). The quantity of dendrimer grown on the MNPs increased with increasing dendrimer generation from 0 to 5.0. The weight losses observed at 800°C on TGA plots show the average weight loss of 4.0%, 7.5%, 11.2%, 17.5%, 22.3%, and 28.5% for the dMNPs (generation 0 to 5.0), respectively. The dendrimer modification process was proven by comparison of FT-IR spectra of the $G_{5.0}$ dMNPs and MNPs. It can be seen from Fig. 2*D* that, compared with the MNPs sample, the $G_{5.0}$ dMNPs possess absorption bands at 2,922 and 2,852 cm^{-1} due to stretching vibration of the C-H bond, bands at 3,422 cm^{-1} due to the bending vibration of the $-NH_2$ group, and bands at 1,719, 1,637, 1,560, and 1,398 cm^{-1} due to the -CO-NH- group. All of these reveal the existence of PAMAM dendrimer.

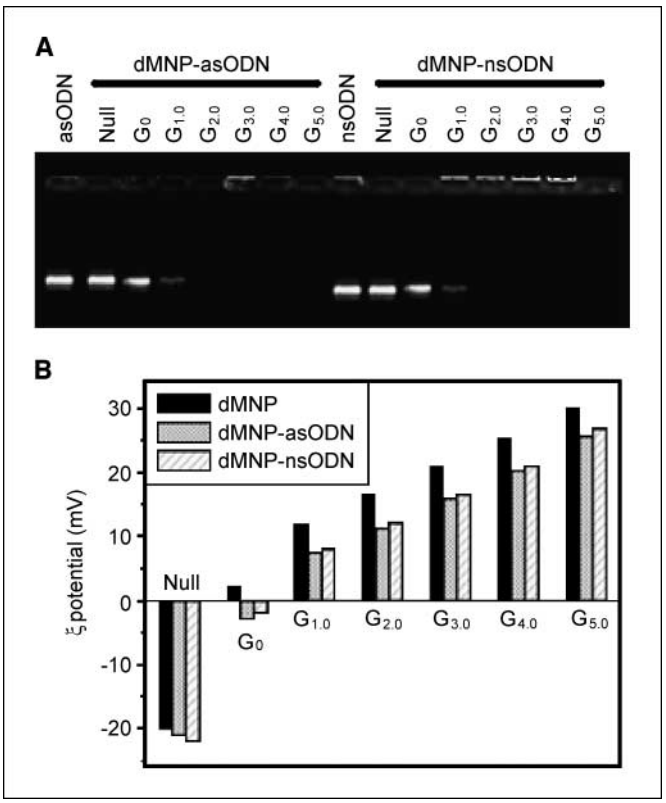

Figure 3. *A,* electrophoretic profile in 1% agarose gel under 365 nm UV light. *B,* ζ potential analysis (pH 7.0) of dMNP-asODN complex (nsODN and null were used as control experiments; null: MNPs without dendrimer modification).

Electrophoretic shift assay and ζ potential analysis. Figure 3*A* shows the electrophoretic shift assay result of asODN in the absence and presence of dMNP with increasing generation from G_0 to $G_{5.0}$, which showed that the amine-terminated dMNP composites could bind with asODN and formed stable dMNP-asODN composites. As shown in Fig. 3*B*, PAMAM dendrimers grown on the surface of MNPs displayed the positive charge properties. The ζ potential of −20 mV at pH 7.0 was observed in MNPs due to the abundant OH^- ions. After MNPs were modified with different generation of dendrimer, ζ potential increased and reached +30 mV at pH 7.0 for $G_{5.0}$ dMNP due to the increasing positive charges of $-NH^{3+}$ on the magnetic surface. There is a statistical difference between surface charge of dMNPs and dMNP-asODN ($P < 0.05$), which showed that lots of positive charges on the surface of dMNPs bind with negative charges on the surface of asODN molecules and form asODN-dMNP composites. As the generation of dendrimer increased, the amount of asODN absorbed by dMNPs also increased correspondingly. $G_{5.0}$ dMNPs absorbed the biggest amount of asODNs. Positively charged asODN-dMNPs will be easily attached to negatively charged cell membrane to improve the endocytosis, so the positively charged surface of asODN-dMNPs is very important for cellular internalization. More positive charges on asODN-dMNP will make higher gene delivery efficiency as shown as follows.

Cell viability and proliferation inhibition assays. As shown in Fig. 4*A*, different generation of dMNPs can inhibit the growth of cancer cells with the inhibition rate of <9%, and as the generation of dendrimer increased, the inhibition rate of cell proliferation caused by dMNPs decreased correspondingly and $G_{5.0}$ dMNPs exhibited lowest toxicology to tumor cells. But no statistical difference of inhibition rates existed among MNPs with $G_{1.0}$ to $G_{5.0}$ generations of dendrimers ($P > 0.05$). The results show that the dMNPs are very low toxic to tumor cells and $G_{5.0}$ dMNP composites exhibited the lowest toxicology to tumor cells.

As shown in Fig. 4*B*, as the generation of dendrimer increased, the inhibition rate of asODN-dMNP composites for tumor cells gradually increased, and there existed statistical difference among different generation of dMNPs ($P < 0.05$). $G_{5.0}$ dMNPs have the highest inhibition rate for tumor cells. Under identical condition, as shown in Fig. 4*C*, the control nsODN-dMNPs also exhibit inhibition effect for tumor cells, but the inhibition rates were markedly lower than those caused by asODN-dMNPs, and there existed a statistical difference between asODN-dMNP group and control nsODN-dMNP group ($P < 0.01$). As shown in Fig. 4*D*, $G_{5.0}$ dMNPs inhibited the growth of tumor cells in dose-dependent means.

Semiquantitative reverse transcription-PCR and Western blot analysis. As shown in Fig. 5*A* and *B*, as the generation of dendrimer increased, the expression levels of gene and protein of *survivin* in tumor cells exhibited gradually down-regulation compared with the control group, and there existed a statistical difference between asODN-dMNP group and nsODN-dMNP group

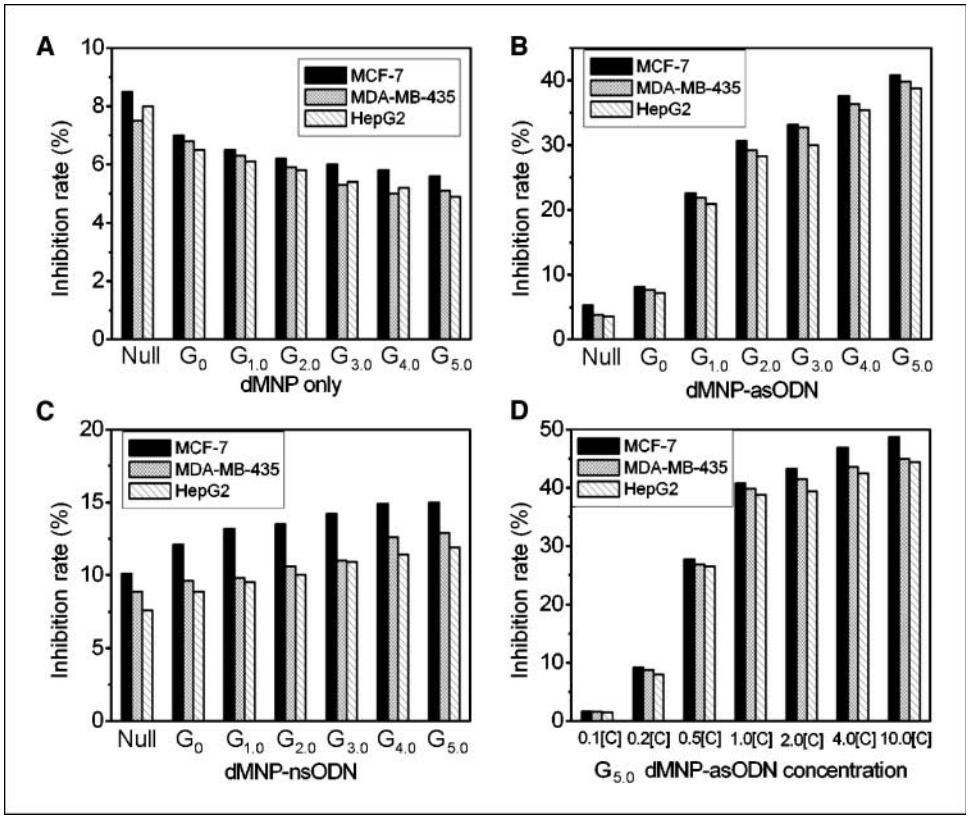

Figure 4. Growth inhibition of cancer cells by dMNP only (*A*), dMNP-asODN (*B*), and dMNP-nsODN (*C*) at different concentration. Concentration = 1.0 [C], incubation time = 72 h; [C] = 0.025 mg/mL dMNP + 2 μmol/L ODN, incubation time = 72 h; null: MNP without dendrimer modification. Growth inhibition of cancer cells by $G_{5.0}$ dMNP-asODN (*D*) at different concentration (null: MNPs without dendrimer modification).

($P < 0.01$) and asODN-$G_{5.0}$ dMNPs exhibited the strongest inhibition effect on expression of *survivin* gene and protein.

Morphologic observation of tumor cells incubated with asODN-dMNPs. Under the identical concentration of dMNP-asODN, as the culture days increased, partial tumor cells gradually became round and suspended and finally exhibited apoptosis or death characterization. To further confirm that the asODN-dMNP nanoparticle conjugates were indeed internalized by the target cells rather than simply bound to the surface of the cells, and to visualize the location of the nanoparticles inside the cells after the internalization, HR-TEM images were taken on MCF-7 cells that were cultured with asODN-dMNP nanoparticles (Fig. 6*A*). HR-TEM images showed that a large number of asODN-dMNP conjugates accumulated on the surface of MCF-7 cells for 0 to 4 h of incubation (Fig. 6*A, a*). After 4 to 12 h of treatment, asODN-dMNP complex entered MCF-7 cells and located within vesicles in the cytoplasm around cell nuclear (Fig. 6*A, b*). The asODN-dMNP complexes appeared as black dots scattered in the cell cytoplasm but not in the nuclei after 12 to 48 h of incubation (Fig. 6*A, c* and *d*), indicating that asODN-dMNP was released from the vesicles and got into the cytoplasm. The complexes cannot enter the nucleus as indicated by HR-TEM characterization. Forty-eight to 96 h of treatment induced cell apoptosis as indicated in Fig. 6*A, e*. Most MCF-7 cells died after incubation with asODN-dMNP for more than 96 h and the ultrastructure was shown in Fig. 6*A, f*. As shown in Fig. 6*B*, asODN-dMNP composites can enter into tumor cells within 15 min of incubation, which fully showed that dMNP composites have high efficiency for delivery of asODN into tumor cells.

As shown in Fig. 6*C*, little changes of fluorescence intensity can be found for control and null sample, whereas the supernatant fluorescence intensity (*curves b, c*, and *d*) decreased markedly after incubating cancer cells with FITC-labeled dMNP-asODN, indicating that dMNP-asODNs were endocytosed by cancer cells. Furthermore, fluorescence intensity decreased with increasing dMNP generation, indicating that the amount of endocytosed asODN-dMNP increased with increasing generation of dMNP from 0 to 5.0. The uptake rate (%) was calculated from Eq. A as shown in Fig. 6*D*. The delivery efficiency (uptake rate) of $G_{5.0}$ dMNP was 60% or so and the delivery efficiency of naked MNPs is 10% or so. There is a statistical difference between the two groups ($P < 0.01$), which showed that dendrimer can improve the across membrane efficiency of MNPs, which also indirectly suggested that dMNPs are likely one kind of good gene delivery system for cancer therapy.

Discussion

Herein, we selected MNPs and dendrimer molecules as raw materials and fabricated dMNP composites and investigated their across membrane efficiency and biological effects with the aim of developing one kind of novel high-efficiency nonviral gene delivery system for cancer therapy. We selected *survivin* asODNs and the control nsODNs as delivery target. $G_{1.0}$ to $G_{5.0}$ dMNP composites were fabricated and characterized by HR-TEM, TGA, and FT-IR. The dMNPs were mixed with asODN and nsODN in the charge ratio of 10:1; under this condition, dMNPs can absorb the maximum oligonucleotides. According to the quality of dendrimer, we can account out the charges of dendrimer surface; therefore, the maximum of asODNs combined with dendrimer can be speculated out—this is one kind of approximate quantitative method. Electrophoretic shift assay and ζ potential analysis also confirmed that there exists statistical difference between surface charge of dMNP and dMNP-asODN, asODN, and nsODN really conjugated

with dMNPs. As the generation of dendrimer increased, the surface charge of dendrimer also increased; therefore, the number of asODN and nsODN combined with the same dMNPs increased correspondingly. $G_{5.0}$ dMNP composites can bind the maximum of oligonucleotides.

To investigate the across cell membrane efficiency of asODN-dMNPs, we used laser confocal microscopy to observe the course of entrance of asODN-dMNPs into MCF-7, MDA-MB-435, HepG2, HL-60, and LNCaP cell line (partial results not shown). Results showed that asODN-dMNPs enter into tumor cells within 15 min of incubation, and asODN-dMNPs were further confirmed to locate some organelles, such as lysosome and endosome, in the cytoplasm by HR-TEM (Fig. 6) similar to other reports (35). According to the measurement method of across membrane efficiency, the delivery efficiency of $G_{5.0}$ dMNPs was 60% or so, the delivery efficiency of naked MNPs is 10% or so, and there is a statistical difference between the two groups ($P < 0.01$), which showed that dendrimer can improve the across membrane efficiency of MNPs, which also indirectly suggested that dMNPs are likely one kind of good gene delivery system for cancer therapy.

To confirm whether antisense *survivin* oligonucleotides in asODN-dMNP composites take effects on MCF-7, MDA-MB-435, and HepG2 cells, we observed that tumor cells with asODN-dMNPs gradually became round and suspended and exhibited apoptosis or death as the culture time increased. Conversely, these cells in the control group without asODN-dMNPs and with dMNPs grew very well. These results showed that antisense *survivin* oligonucleotides in asODN-dMNP composites took effects against cell proliferation. To further confirm this point, semiquantitative reverse transcription-PCR (RT-PCR) and Western blot were used to detect the expression levels of *survivin* gene/protein in tumor cells. Result showed that *survivin* gene/protein in MCF-7, MDA-MB-435, and HepG2 cells with asODN exhibited gradually down-regulation expression as the dose of asODN-dMNPs and culture time increased; conversely, these cells in the control group exhibited no marked change in expression of *survivin* gene and protein. Similar results also were observed for HL-60 cells and human prostate cancer LNCaP cell line (data not shown). These results fully showed that asODN of asODN-dMNPs can bind with start site of *survivin* mRNA and block translation of *survivin* mRNA into *survivin* protein and finally down-regulated expression of *survivin* gene and protein. These results also showed that dMNPs do not affect the function of antisense *survivin* oligonucleotides in tumor cells. There is one interesting question, that is, in the course of antisense *survivin* oligonucleotides blocking translation of *survivin* mRNA into protein in tumor cells, asODN escaped from asODN-dMNPs and then took effect or asODN-dMNPs as a whole unit took effects? We consider that, first, asODN can escape from asODN-dMNPs under the cell *in vivo* environment and then asODNs themselves bind with start site of *survivin* mRNA and block translation of *survivin* mRNA into *survivin* protein. The dMNPs may be expelled out of cells. The concrete course and mechanism still need further clarification.

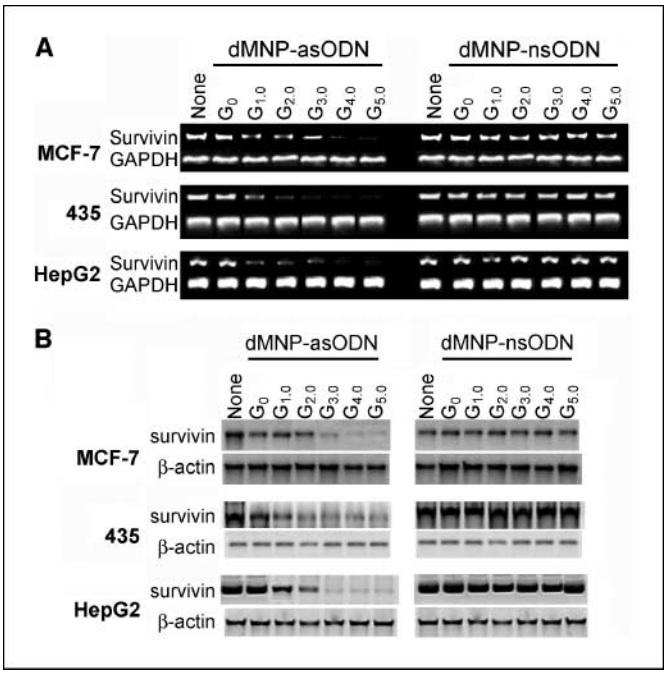

Figure 5. The effect of dMNPs-asODN against *survivin* on *survivin* expression in MCF-7, MDA-MB-435, and HepG2 cells. dMNP-asODN transfection was done at 3,000 patients/cell. *A,* RT-PCR analysis of *survivin* or GAPDH (internal control) mRNA expression done 72 h after transfection. *B,* Western blot analysis of *survivin* or β-actin (internal control) protein expression done 72 h after transfection (none: without adding dMNP-asODN).

Using dMNPs as the gene nanovector may prevent fast degradation of the asODN by enzymes *in vivo* cells (36) and extend the lifetime of asODN inside cells (37, 38). Because dMNPs can change the cellular microenvironment within a short time, absorbed some ions, and change the pH of the environment, they can protect asODN from degradation caused by *in vivo* enzymes (35, 39, 40). Lots of research reports showed that antisense oligonucleotides take effects within 2 days after entering into tumor cells. As the time increases, the function of asODN will disappear gradually (15–17). In this study, we observed that, as the incubation day increased, the cell growth inhibition became more and more marked, and at no. 5 day, the inhibition effects reach high peak. Therefore, we consider that dMNPs may be helpful to protect antisense oligonucleotides from fast degradation by enzymes *in vivo*. The concrete mechanism still needs further clarification.

According to above-mentioned results, we suggest a possible model of interaction between asODN-dMNPs and tumor cells (Fig. 1). The asODNs combined with dMNPs via electrostatic means; the resulting asODN-dMNP nanocomposites have positive charge on their surface, easily attached to the surface of tumor cells (24, 25), induced internalization of asODN-dMNPs into tumor cells by endocytosis means (26) under the action of lysosome enzymes and ions in cells; and asODN escaped from asODN-dMNP composites, enter into ribosome (8, 12, 13), bind the start sites of *survivin* mRNA, block translation of *survivin* mRNA into *survivin* protein, eliminate the function of *survivin* protein against apoptosis, and induced cell apoptosis. The dMNPs may be expelled from *in vivo* of cells.

In conclusion, different generation of dendrimer-conjugated MNPs are successfully fabricated, and these resulting dendrimer-MNP composites can bind with antisense *survivin* oligonucleotides via electrostatic means. The amount of combined antisense *survivin* oligonucleotides increases accordingly as the generation of dendrimer increases, and dendrimer coating layer markedly improves the solubility of MNPs. The asODN-dMNP composites can cross cell membrane and enter into tumor cells within 15 min and inhibit the growth of tumor cells. The dMNPs almost do not affect the growth of tumor cells and are helpful to protect asODN

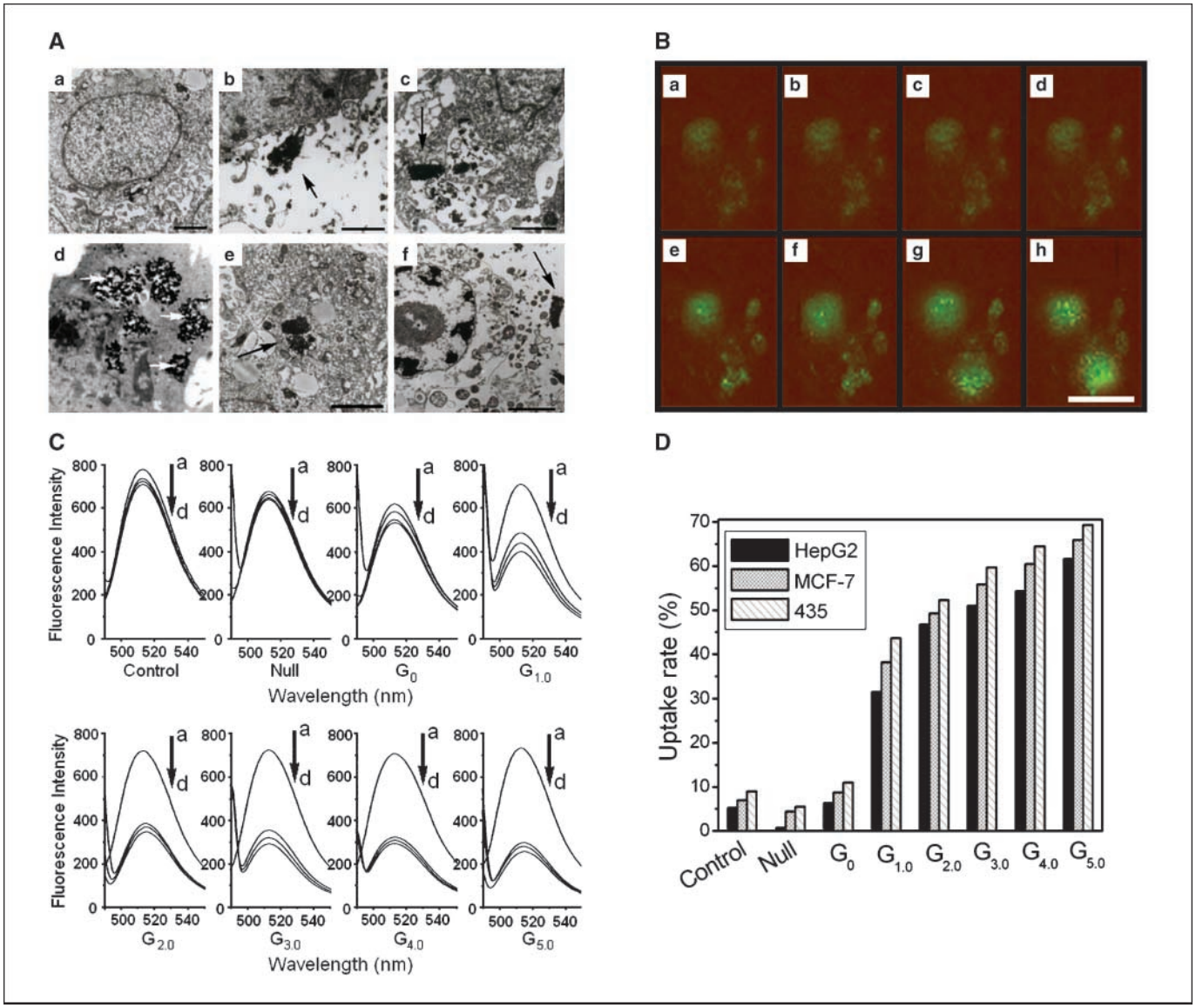

Figure 6. *A,* ultrastructure observation of MCF-7 cells from HR-TEM microscopy. MCF-7 cells incubated with no dMNP-asODN (*a*) and asODN-$G_{5.0}$ dMNP complex (2 μmol/L + 0.025 mg/mL) for 0 to 4 h (*b*), 4 to 12 h (*c*), 12 to 24 h and 24 to 48 h (*d*), 48 to 96 h (*e*), and more than 96 h (*f*), indicating cell apoptosis induced by dMNP-asODN complex. *Bar,* 500 nm. *B,* confocal laser microscopy of MCF-7 cells incubated with FITC-asODN-$G_{5.0}$ dMNP (2 μmol/L + 0.025 mg/mL) for 1 min (*a*), 3 min (*b*), 5 min (*c*), 7 min (*d*), 10 min (*e*), 15 min (*f*), 20 min (*g*), and 30 min (*h*). *Bar,* 10 μm. *C,* fluorescence intensity of cell culture medium supernatant after cell incubation with dMNP-FITC-asODN. Fluorescence of the same medium without cell culture was also detected as control (*a*), HepG2 (*b*), MDA-MB-435 (*c*), and MCF-7 (*d*). *D,* intracellular uptake rate of dMNP-asODN (control: without dMNP; null: MNP without dendrimer modification).

from degradation by enzymes inside cells and almost do not affect the function of asODN in cells. The asODN-$G_{5.0}$ dMNPs exhibit the maximum inhibition against tumor cell growth. Although the concrete metabolism of asODN-MNPs inside cells still is not clear, the dendrimer-conjugated MNPs may be one kind of generic high-efficiency gene delivery system and have potential application in delivery of gene or drug for cancer therapy.

Acknowledgments

Received 12/27/2006; revised 5/21/2007; accepted 6/20/2007.

Grant support: China National 973 Project No. 2005CB723400-G, 863 Project No. 2007AA022003, National Natural Scientific Fund No. 30471599, Pujiang Plan Project No. 06PJ14049, and Shanghai Fund of Scientific and Technology No. 054119527.

The costs of publication of this article were defrayed in part by the payment of page charges. This article must therefore be hereby marked *advertisement* in accordance with 18 U.S.C. Section 1734 solely to indicate this fact.

References

1. Salem AK, Searson PC, Leong KW. Multifunctional nanorods for gene delivery. Nat Mater 2003;2:668–71.
2. Sengupta S, Eavarone D, Capila I, et al. Temporal targeting of tumour cells and neovasculature with a nanoscale delivery system. Nature 2005;436:568–72.
3. Pack DW, Hoffman AS, Pun S, Stayton PS. Design and development of polymers for gene delivery. Nat Rev Drug Discov 2005;4:581–93.
4. Cai D, Mataraza JM, Qin Z, et al. Highly efficient molecular delivery into mammalian cells using carbon nanotube spearing. Nat Methods 2005;2:449–54.
5. Hütten A, Sudfeld D, Ennen I, et al. New magnetic nanoparticles for biotechnology. J Biotechnol 2004;112:47–63.
6. Ito A, Shinkai M, Honda H, Kobayashi T. Medical

application of functionalized magnetic nanoparticles. J Biosci Bioeng 2005;100:1–11.
7. Won J, Kim M, Yi YW, Kim YH, Jung N, Kim TK. A magnetic nanoprobe technology for detecting molecular interactions in live cells. Science 2005;309:121–5.
8. Kim DH, Lee SH, Kim KN, Kim KM, Shim IB, Lee YK. Cytotoxicity of ferrite particles by MTT and agar diffusion methods for hyperthermic application. J Magn Magn Mater 2005;293:287–92.
9. Lee H, Lee E, Kim DK, Jang NK, Jeong YY, Jon S. Antibiofouling polymer-coated superparamagnetic iron oxide nanoparticles as potential magnetic resonance contrast agents for *in vivo* cancer imaging. J Am Chem Soc 2006;128:7383–9.
10. Ito A, Ino K, Kobayashi T, Honda H. The effect of RGD peptide-conjugated magnetite cationic liposomes on cell growth and cell sheet harvesting. Biomaterials 2005;26:6185–93.
11. Sincai M, Ganga D, Ganga M, Argherie D, Bica D. Antitumor effect of magnetite nanoparticles in cat mammary adenocarcinoma. J Magn Magn Mater 2005; 293:438–41.
12. Morishita N, Nakagami H, Morishita R, et al. Magnetic nanoparticles with surface modification enhanced gene delivery of HVJ-E vector. Biochem Biophys Res Commun 2005;334:1121–6.
13. Guedes MHA, Sadeghiani N, Peixoto DLG, et al. Effects of AC magnetic field and carboxymethyldextran-coated magnetite nanoparticles on mice peritoneal cells. J Magn Magn Mater 2005;293:283–6.
14. Cui D, Tian F, Coyer CR, et al. Effects of antisense-Myc conjugated single walled carbon nanotubes on HL-60 cells. J Nanosci Nanotechnol 2007;7:1639–46.
15. Yang DI, Chen S, Ezekiel UR, Xu J, Wu Y, Hsu CY. Antisense RNA to inducible nitric oxide synthase reduces cytokine-mediated brain endothelial cell death. Ann N Y Acad Sci 2005;1042:439–47.
16. Ching JL, Mulligan RC, Schimmel P, Holmes EW. Antisense RNA complementary to 3′ coding and non-coding sequences of creatine kinase is a potent inhibitor of translation *in vivo*. Proc Natl Acad Sci U S A 1989;86: 10006–10.
17. Denhardt DT. Mechanism of action of antisense RNA. Sometime inhibition of transcription, processing, transport, or translation. Ann N Y Acad Sci 1992;660: 70–6.
18. Holt JT. Antisense promoter mapping. Inhibitory methods of transcriptional analysis. Ann N Y Acad Sci 1992;66:88–94.
19. Tarkanyi I, Horvath A, Szatmari I, et al. Inhibition of human telomerase by oligonucleotide chimeras, composed of an antisense moiety and a chemically modified homo-oligonucleotide. FEBS Lett 2005;579:1411–6.
20. Shadidi M, Sioud M. Identification of novel carrier peptides for the specific delivery of therapeutics into cancer cells. FASEB J 2003;17:256–8.
21. Bonora GM, Ivanova E, Zarytova V, Burcovich B, Veronese FM. Synthesis and characterization of high-molecular mass polyethylene glycol-conjugated oligonucleotides. Bioconjug Chem 1997;8:793–7.
22. Lee JW, Kim BK, Kim HJ, Han SC, Shin WS, Jin SH. Convergent synthesis of symmetrical and unsymmetrical PAMAM dendrimers. Macromolecules 2006;39: 2418–22.
23. Hong S, Leroueil PR, Janus EK, et al. Interaction of polycationic polymers with supported lipid bilayers and cells: nanoscale hole formation and enhanced membrane permeability. Bioconjug Chem 2006;17:728–34.
24. Majoros IJ, Myc A, Thomas T, Mehta CB, Baker JR. PAMAM dendrimer-based multifunctional conjugate for cancer therapy: synthesis, characterization, and functionality. Biomacromolecules 2006;7:572–9.
25. Radu DR, Lai CY, Jeftinija K, Rowe EW, Jeftinija S, Lin VSY. A polyamidoamine dendrimer-capped mesoporous silica nanosphere-based gene transfection reagent. J Am Chem Soc 2004;126:13216–7.
26. Majoros IJ, Thomas TP, Mehta CB, Baker JR. Poly(amidoamine) dendrimer-based multifunctional engineered nanodevice for cancer therapy. J Med Chem 2005;48:5892–9.
27. Pan B, Gao F, Ao L. Investigation of interactions between dendrimer-coated magnetite nanoparticles and bovine serum albumin. J Magn Magn Mater 2005;293: 252–8.
28. Pan B, Cui D, Gao F, He R. Growth of multi-amine terminated poly(amidoamine) dendrimers on the surface of carbon nanotubes. Nanotechnology 2006;17: 2483–9.
29. Pan B, Gao F, Gu H. Dendrimer modified magnetite nanoparticles for protein immobilization. J Colloid Interface Sci 2005;284:1–6.
30. Sun C, Nettesheim C, Liu Z, Olejniczak ET. Solution structure of human *survivin* and its binding interface with smac/diablo. Biochemistry 2005;44:11–7.
31. Fuessel S, Herrmann J, Ning S, et al. Chemosensitization of bladder cancer cells by *survivin*-directed antisense oligodeoxynucleotides and siRNA. Cancer Lett 2006;232:243–54.
32. Kim SH, Mok H, Jeong HJ, Kim SW, Park TG. Comparative evaluation of target-specific GFP gene silencing efficiencies for antisense ODN, synthetic siRNA, and siRNA plasmid complexed with PEI-PEG-FOL conjugate. Bioconjug Chem 2006;17:241–4.
33. Cui D, Tian F, Wang M, Ozkan CS, Gao H. Effects of single walled carbon nanotubes on HEK293 cells. Toxicol Lett 2005;115:73–85.
34. Cui D, Jin G, Gao T, et al. Characterization of BRCAA1 and its novel antigen epitope identification. Cancer Epidemiol Biomarkers Prev 2004;13:1136–45.
35. Han Y, Huan Y, Deng J, Gao F, Pan B, Cui D. Expression of single-chain Fv gene specific for γ-seminoprotein by RTS and its biological activity identification. Biotechnol Prog 2006;22:1084–9.
36. Zhang Z, Cao X, Zhao X, et al. Controlled delivery of antisense oligodeoxynucleotide from cationically modified phosphorylcholine polymer films. Biomacromolecules 2006;7:784–91.
37. Cui D. Advance and prospect of biomolecules functionalized carbon nanotubes. J Nanosci Nanotechnol 2007;7:1298–314.
38. Chang E, Yu WW, Colvin VL, Drezek R. Quantifying the influence of surface coatings on quantum dot uptake in cells. J Biomed Nanotechnol 2005;1: 397–401.
39. Smith AM, Duan H, Rhyner MN, Ruan G, Nie S. A systematic examination of surface coatings on the optical and chemical properties of semiconductor quantum dots. Phys Chem Chem Phys 2006;8:3895–903.
40. Gupta AK, Naregalkar RR, Vaidya VD, Gupta M. Recent advances on surface engineering of magnetic iron oxide nanoparticles and their biomedical applications. Nanomedicine 2007;2:23–39.

Dendrimer-Modified Magnetic Nanoparticles Enhance Efficiency of Gene Delivery System

Bifeng Pan, Daxiang Cui, Yuan Sheng, et al.

Cancer Res 2007;67:8156-8163.